# Effect of Sinusoidal Excitation on the Chua's Circuit

K. Murali and M. Lakshmanan

*Abstract*—**We examine the effect of an external periodic excitation on the Chua's piecewise-linear circuit. Under the action of such a force this circuit exhibits a large variety of bifurcation sequences, including period-doubling, period-adding, and windows in chaos regime. In addition, at certain parameters equal periodic bifurcations, hysteresis, quasi-periodic, and intermittent behaviors and coexistence of multiple attractors have also been observed. A bifurcation diagram that classifies the attractors in the forcing parameters plane is presented.**

## I. Introduction

In recent times a great deal of interest has been focused on exploring complexity of nonlinear circuits and dynamical systems [1], [2]. Observations of different properties such as period-doubling bifurcations, period-adding sequences, quasi-periodicity and intermittent transitions have been studied in a number of different physical circuits and systems. In this connection one of the most prominently and extensively investigated circuit is Chua's piecewise-linear circuit [3], [4].

A number of experimental, numerical and theoretical investigations have been carried out on this circuit to study the nature of chaos for various parametric choices [3], [4]. However, up to now, the nonautonomous version of this circuit seems not to have been explored, as far as the authors' knowledge goes. Since nonautonomous versions can give rise to a rich variety of nonlinear phenomena, the emphasis of this paper is on the effect of an external periodic excitation on the Chua's autonomous circuit. The resultant study reveals a very rich variety of bifurcation sequences. In a recent report [5], we briefly pointed out the observation of many bifurcation sequences in the nonautonomous circuit for certain parametric choices. Presently, we have performed a detailed investigation on the dynamics of this circuit to observe an immense variety of bifurcation sequences such as period-adding, quasi-periodicity, intermittency, equal periodic bifurcations, hysteresis, and coexistence of multiple attractors in phase-space besides the standard bifurcation sequences. Thus this simple circuit alone is seen to possess almost all the bifurcation sequences reported to date. Due to the simplicity and rich content of nonlinear dynamical phenomena, under the environment of external periodic signal, Chua's circuit can be viewed as a black box to study almost all bifurcation sequences reported so far.

Manuscript received November 13, 1990. This work was supported by the Department of Atomic Energy of the Government of India, through a research fellowship awarded to K. Murali. This paper was recommended by Associate Editor H.-D. Chiang.

The authors are with the Centre for Nonlinear Dynamics, Department of Physics, Bharathidasan University, Tiruchirapalli, 620 024, India.

IEEE Log Number 9105223.

## II. Experimental Setup and Results

### A. The Circuit

The experimental circuit that we have employed is shown in Fig. 1. Here $L_1$, $L_2$, $C_1$, $C_2$, and $R$ are all linear passive components. This circuit contains only one nonlinear element: a nonlinear-resistor (subcircuit $N$) whose function curve $i_R - V_R$ is shown in Fig. 2, which is piecewise-linear in nature. It is straightforward to see that the dynamics can be modeled by the following equations:

$$
\begin{aligned}
C_1 \frac{dV_{C1}}{dt} &= \frac{1}{R}(V_{C2} - V_{C1}) - g(V_{C1}) \\
C_2 \frac{dV_{C2}}{dt} &= \frac{1}{R}(V_{C1} - V_{C2}) + i_{L2} - i_{L1} \\
L_1 \frac{di_{L1}}{dt} &= V_{C2} - F\sin(\omega t) \\
L_2 \frac{di_{L1}}{dt} &= -V_{C2} \qquad (1)
\end{aligned}
$$

where $V_{C1}$, $V_{C2}$, $i_{L1}$, and $i_{L2}$ are the voltage across $C_1$, the voltage across $C_2$, the current through $L_1$, and the current through $L_2$, respectively. Here $F\sin(\omega t)$ is the external forcing source. $g(V_{C1})$ is the piecewise-linear function having its functional representation [6] as

$$
g(V_{C1}) = m_0 V_{C1} + (1/2)(m_1 - m_0) \cdot (|V_{C1} + B_P| - |V_{C1} - B_P|) \qquad (2)
$$

where $m_0$ is the slope of the first and last segments and $m_1$ is the slope of the middle segment of the functional curve of the nonlinear resistor as shown in Fig. 2. Here, $B_P$ is the break point voltage. When the second inductor $(L_2)$ is absent and the external force is zero in the circuit in Fig. 1, we have the standard Chua's autonomous circuit. This version admits period-doubling bifurcations and double-scroll chaotic attractor for certain ranges of parameter values [3], [4]. One can introduce the external periodic signal in series with inductor $L_1$ and study the dynamics of (1). However, for the range of parametric values we have studied, it admits no new bifurcation phenomena other than the ones admitted by the autonomous version. We have therefore included one more passive element $(L_2)$ as shown in Fig. 1 and investigated the underlying dynamics.

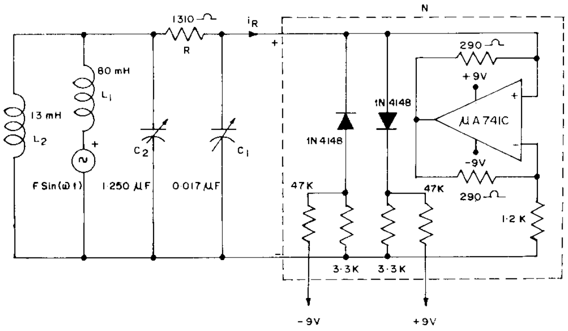


Fig. 1. Electronic circuit representing the driven piecewise-linear system.

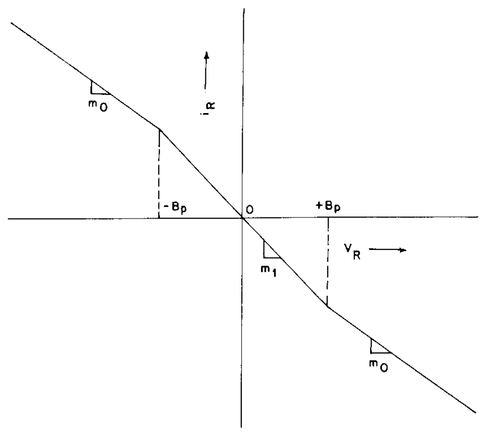


Fig. 2. V-I characteristics of the nonlinear resistor.

Now the behavior of the circuit depends on the parameters $C_1$, $C_2$, $L_1$, $L_2$, $R$, the amplitude $F$, and the frequency $f(=\omega/2\pi)$ of the external forcing source. In the present study we carried out the experiment by fixing all the parameters as in Fig. 1 except the external driving source parameters. We varied the amplitude $F$ from 0 to 800 mV(rms) and the frequency $f$ from 800 to 1300 Hz to study the bifurcation sequences. It may be noted that for the present circuit parameters, the autonomous case $F = 0$, corresponds to the usual fixed point attractor.

### B. The Bifurcation Diagram

Based on our extensive measurements of voltage changes across the capacitors $C_1$ and $C_2$ and the associated transition to chaos with different forcing parameter values, a profile of bifurcation diagram in the $(F-f)$-plane has been constructed as shown in Fig. 3. This figure exhibits the kind of oscillations that the circuit admits, for each value of the driving amplitude $F$ and frequency $f$. We traced the waveforms of voltage $V_{C1}$ across $C_1$ and voltage $V_{C2}$ across $C_2$, which are the two signals under surveillance to study the bifurcation sequences. We have noted the changes in the attractor projected onto the $(V_{C1} - V_{C2})$-plane directly on the oscilloscope. A Poincaré map circuit as shown in Fig. 4 has been employed to produce a live picture of the strobed

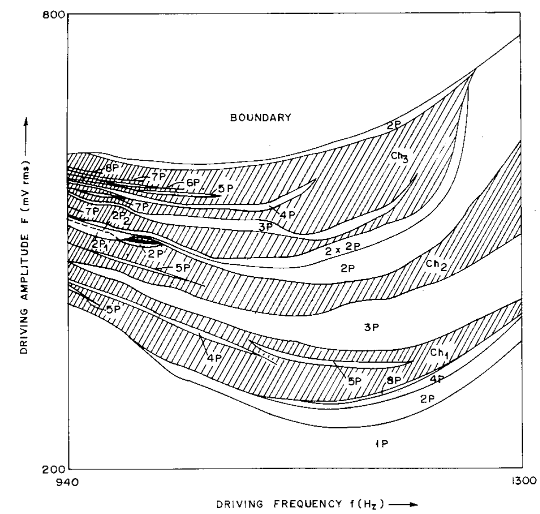


Fig. 3. Bifurcation diagram in $F$-$f$ plane. Numbers are the period of the attractors. Shaded regions express the chaos.

Poincaré map of the projected attractor, that is, by triggering the beam of the oscilloscope at the driving source frequency $f(=\omega/2\pi)$ ($Z$-modulation). In Fig. 3, the numbers indicate the period of the observed attractors and the shaded regions indicate chaos.

### C. Period-Doubling Scenario

For the experimental circuit, when the drive voltage ($F$) is small, only period-one motion synchronized with the external signal takes place. For $F = 0$, only fixed point motion is observed. As $F$ is increased from 0 mV, Hopf bifurcation initially occurs, and beyond $F = 200$ mV, the system undergoes a cascade of period-doubling bifurcations in the middle of the frequency region (see Fig. 3). These bifurcation sequences can be easily identified either by direct observation of the projected attractor or by the observation of the Poincaré map displayed on the oscilloscope. As the order of the period in the period-doubling sequence increases, the difference between the drive voltage ($F$) corresponding to two successive bifurcations becomes smaller. The calculated convergence rates are close to the Feigenbaum's constants. Also, there are some periodic windows appearing within the chaotic regimes. Further period-doubling of these basic windows is too narrow and therefore is not indicated in Fig. 3.

A typical chaotic attractor projected onto the $(V_{C1} - V_{C2})$-plane and its corresponding Poincaré map in the region $Ch_2$ are depicted in Fig. 5. However, for higher drive amplitude values, beyond the chaotic region $Ch_3$, boundary crisis is usually observed. Also, at lower drive amplitude values, one can observe period-halving or reverse period-doubling bifurcations upon increasing or decreasing the forcing frequency values at fixed drive amplitudes.

### D. Period Adding Scenario

Recently, the period adding sequence has been reported in some driven negative resistance oscillators [7], [8]. In these studies a complicated succession of periodic and chaotic

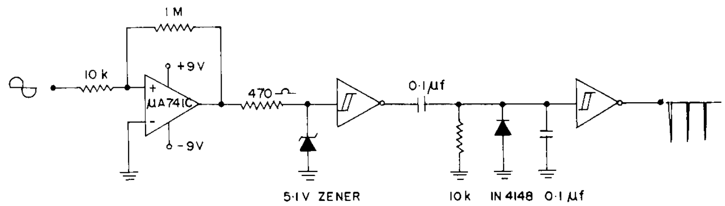


Fig. 4. Strobed Poincaré map circuit.

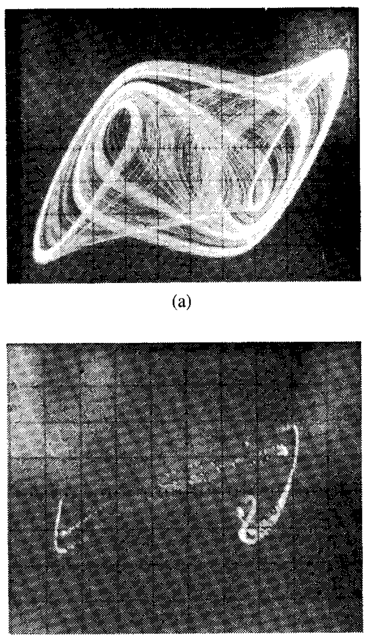

(a)

(b)

Fig. 5. (a) Typical chaotic attractor projected onto the $V_{C1} - V_{C2}$ plane in the $Ch_2$ region for $F = 500$ mV and $f = 1200$ Hz. (b) Strobed Poincaré map of Fig. 5(a).

oscillations have been experimentally observed. During our experiments with the present circuit, we observed periodic windows of all orders from period-2 to period-8 in addition to the period-doubling cascades to chaos. Although we have noticed up to period-12 window in the period-adding sequence, it is difficult to observe higher period windows since the separation between successive window regions decreases and the width of the window regions diminishes. If we look at Fig. 3, for higher drive amplitude values a succession of large periodic windows whose period increase exactly by one appears, as we move from one window to the next, as the drive amplitude is increased. These windows are found to satisfy the Farey sequence [9]. In the chaos region $Ch_1$ between $3P$ and $2P$ window regimes, there is a $5P$ window($= 3 + 2$); between $3P$ and $1P$ there is $4P(= 3 + 1)$ and between $4P$ and $1P$ there is $5P(= 4 + 1)$. Also, a period $7P$ window($= 3 + 4$) appears in the chaos region $Ch_3$.

In the period adding sequence, each periodic window is found to persist over a limited range of forcing parameter($F$) values, thereby creating a step-like bifurcation diagram where the forcing amplitude ($F$) versus the period of the observed window is plotted. In order to elucidate this structure the period diagram for $f = 941$ Hz is shown in Fig. 6. The transition from one periodic state to another is initiated by a period-doubling bifurcation to chaos followed by recovery to the next periodic state in the period adding structure.

### *E. Quasi-periodic and Intermittent Behavior*

In some nonlinear dynamical systems and circuits [10]–[13] quasi-periodic and intermittent transitions have been reported recently. In the present study, however, quasi-periodic motions have been observed in the regions of lower drive amplitude ($F$) and frequency ($f$) values. A typical quasi-periodic attractor for $F = 516.9$ mV, $f = 820$ Hz is depicted in Fig. 7. In these regions, small rotating circles are observed on the Poincaré map. Also, some portions of the trajectory plot in the $V_{C1} - V_{C2}$ plane rotate smoothly in a clockwise direction, signalling the quasi-periodic state [10]. As the forcing parameter is varied slowly, the quasi-periodic motion breaks up and chaotic motion sets in.

Also, beyond some critical forcing parameters the system transits to intermittent regions. During this motion irregular bursts of chaos are interspersed with stable periodic window regions (laminar phases) lasting a variable length of time. Fig. 8(a) depicts a typical trajectory plot in $V_{C1} - V_{C2}$ plane for an intermittency region near period-2 window region ($F = 589.7$ mV and $f = 840$ Hz). For a long time exposure the trace is continuous, indicating a chaotic behavior. A portion of the time dependence of waveform $V_{C1}$ corresponding to Fig. 8(a) is shown in Fig. 8(b), where the periodic oscillations are interrupted by intermittent voltage bursts. Also near the boundary crisis [11] region beyond the period-adding structure the waveform or the attractors are dominated by the intermittency. A typical trajectory plot in $V_{C1} - V_{C2}$ plane with intermittent transitions near the boundary crisis point is shown in Fig. 9(a) and a portion of the time dependence of waveform $V_{C1}$ corresponding to Fig. 9(a) is shown in Fig. 9(b), for $F = 620$ mV and $f = 941$ Hz. In these intermittent transition behaviors, the signal $V_{C1}$ or $V_{C2}$ loses its regularity and chaotic burst appears at a particular subharmonic amplitude together with a decrease (or increase) of the fundamental amplitude. Immediately after this there is a reappearance of the regular (laminar) behavior. This type of intermittency is normally classified as type-III [12], [13]. One can also confirm this by plotting the return maps ($V_{C1,n}$ versus $V_{C1,(n+1)}$ or $V_{C2,n}$ versus $V_{C2,(n+1)}$).

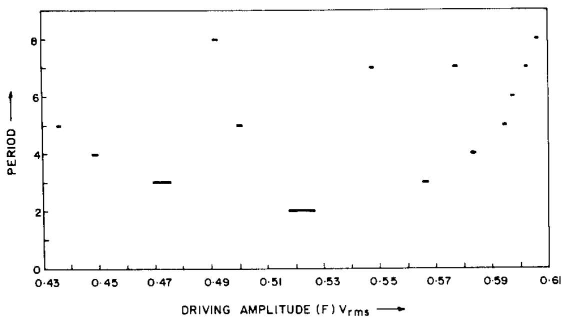


Fig. 6. Period diagram showing the period-adding structure for $f =$ 941 Hz.

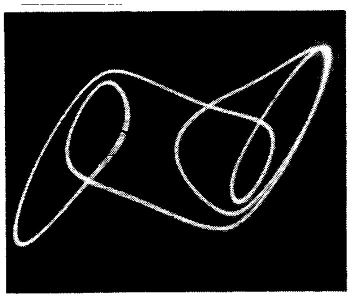

(a)

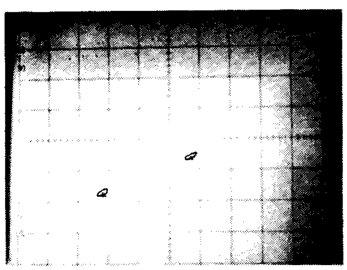

(b)

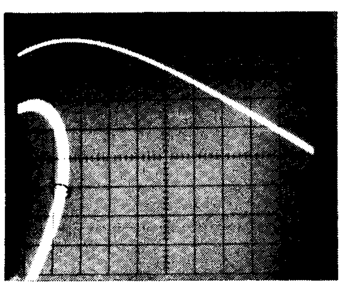

(c)

Fig. 7. Quasi-periodic attractor for $F = 516.9$ mV and $f = 820$ Hz. (a) Trajectory plot in $V_{C1} - V_{C2}$ plane. (b) The Poincaré map of (a). (c) Enlargement of a portion of (a). Trajectories are found to rotate in the direction as indicated by the arrow.

## F. Equal Periodic or Period Preserving Bifurcation

The study of equal periodic bifurcation or period preserving bifurcation is of considerable interest [14]. In a typical two-dimensional area preserving map, if the control parameter is larger than some critical value, the original periodic motion is nonstationary and two new periodic motions appear together with the same period as the original one [14]. This phenomenon is called equal periodic bifurcation and it is recently reported in some dissipative dynamical systems.

Let us look at the period-2 window within the chaos regime $Ch_2$ and $Ch_3$ in Fig. 3. There are two regions $2P_1$ and $2P_2$ divided by a dotted line for certain forcing parame-

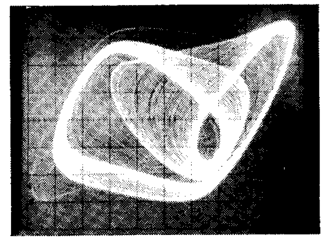

(a)

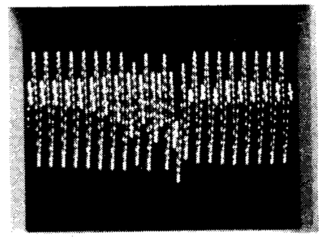

(b)

Fig. 8. (a) Trajectory plot in $(V_{C1} - V_{C2})$ plane for an intermittency region ($F = 589.7$ mV, $f = 840$ Hz). (b) Portion of waveform $(V_{C1})$ with parameters same as Fig. 8(a).

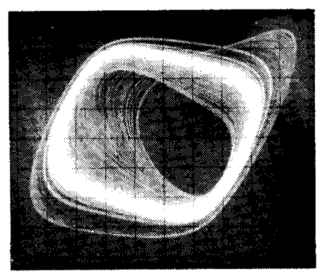

(a)

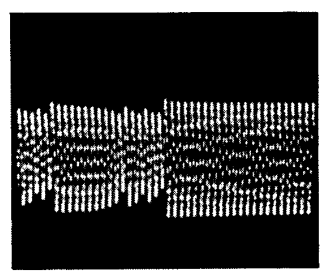

(b)

Fig. 9. (a) Trajectory plot in $(V_{C1} - V_{C2})$ plane for an intermittency region near boundary crisis region for $F = 620$ mV, $f = 941$ Hz. (b) Portion of waveform $(V_{C1})$ with parameters same as Fig. 9(a).

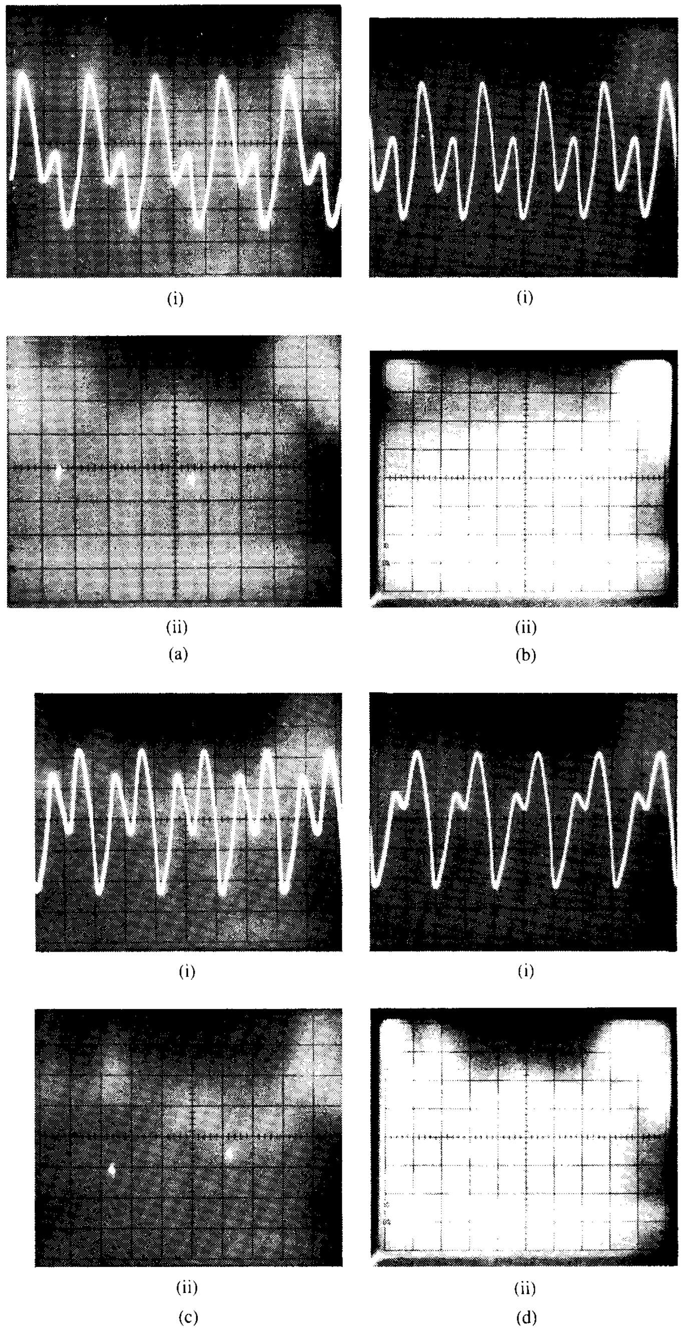


Fig. 10. (a) i) The waveform ($V_{C1}$) and ii) strobbed Poincaré map of $2P_1$ region ($F = 518.6$ mV, $f = 940$ Hz). (b) Same as Fig. 10(a) for $2P_1$ region ($F = 523.3$ mV, $f = 940$ Hz). (c) Same as Fig. 10(a) for $2P_2$ region ($F = 524.7$ mV, $f = 940$ Hz). (d) Same as Fig. 10(a) for $2P_2$ region ($F = 522.9$ mV, $f = 940$ Hz).

ter values and a single $2P$ region for another set of parameters. For example, if we choose $f = 940$ Hz, initially for $F = 518.6$ mV, the $2P_1$ structure of Fig. 10(a) appears. This structure slightly changes as in Fig. 10(b) for $F = 523.3$ mV. Further increase of $F$ value gives birth to $2P_2$ structure as in Fig. 10(c), and it appears up to $F = 524.7$ mV. Here both the $2P_1$ and $2P_2$ structures have the same period two but their waveforms ($V_{C1}$ or $V_{C2}$) and their corresponding Poincaré sections ($V_{C1} - V_{C2}$ plane) look different.

An important point here is that there can be a $2P_1$ or $2P_2$ structure depending on the initial conditions in the area near the dotted line in Fig. 3. For example, if we initially cut off the external sinusoidal source and connect it instantly to the circuit, then either of the $2P_1$ or $2P_2$ oscillations appear

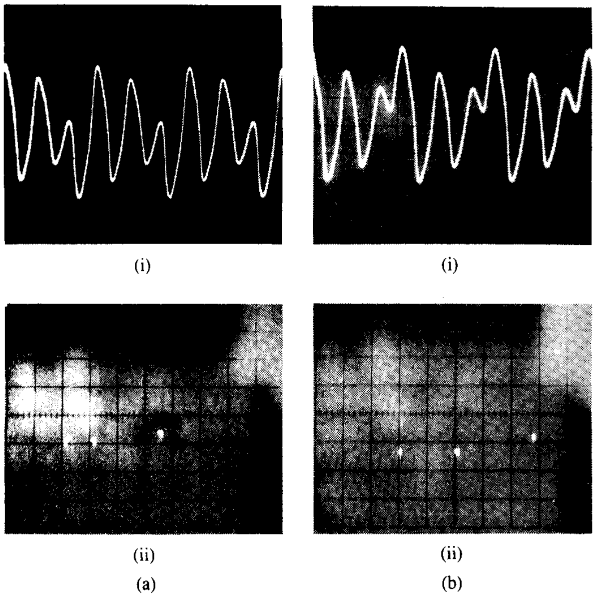


Fig. 11. (a) Same as Fig. 10(a) for $3P_1$ region ($F$ = 594.6 mV, $f$ = 880 Hz). (b) Same as Fig. 10(a) for $3P_2$ region ($F$ = 600.8 mV, $f$ = 880 Hz).

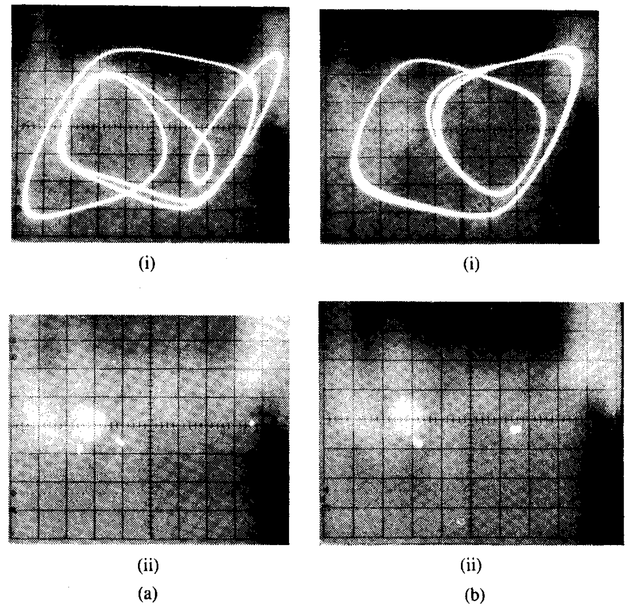


Fig. 12. Coexistence of attractors for F = 587.2 mV, f = 840 Hz. (a) i) Period-4 attractor; ii) Poincaré map of i). (b) i) Chaotic attractor; ii) Poincaré map of i).

randomly, but it is quite unpredictable. It is interesting to note that further change in the value of $F$ after the equal periodic bifurcation gives birth to period-doubling bifurcation in period-$2P_2$ region. Further, the system also exhibits period-doubling bifurcations from $2P_1$ to $4P$, etc. for the set of parameters ($F$ and $f$) in the $2P_1$ region. Also, a similar kind of equal periodic bifurcation has been observed in small area of period-3 window region in the area $Ch_3$ for $F$ = 594.6 mV, $f$ = 880 Hz (Fig. 11(a)) and $F$ = 600.8 mV, $f$ = 880 Hz (Fig. 11(b)), respectively.

### G. Hysteresis Jumps and Coexistence of Multiple Attractors

We have also observed the hysteresis phenomenon in our experiments, but they do not seem to have any influence over the equal periodic bifurcation. As discussed in the previous section, within the equal periodic bifurcation region, the transition from $2P_1$ structure (Fig. 10(a)) to $2P_2$ structure (Fig. 10(c)) is observed by increasing the amplitude $F$ with fixed frequency $f$ = 940 Hz. However, the structure of Fig. 10(b) is not recovered by resetting the value of $F$, that is, the transition path is irreversible. Even if we decrease the $F$ value from 524.7 mV, the $2P_2$ structure of Fig. 10(c) persists initially and a slightly changed structure of Fig. 10(d) is observed for $F$ = 522.9 mV. On small decrease of $F$ value below 522.9 mV, the $2P_1$ structure of Fig. 10(a) is observed instead of Fig. 10(b). Thus the system follows a different transition path while $F$ is decreased rather than $F$ is increased, reminiscent of a hysteresis [11], [15]. Even during this transition, the system still possesses equal periodic bifurcation. This kind of hysteresis transition has also been observed in the period-3 window region of the $Ch_3$ area.

For nonlinear dissipative dynamical systems, two or more attractors may coexist in phase-space; that is, more than one dynamical behavior is possible, depending solely on the initial conditions. Recently, coexistence of multiple attractors have been reported in some dynamical systems [15], [16]. In the following we report the coexistence of periodic and chaotic attractor in the present circuit. Fig. 12 depicts the coexistence of a period-4 and a chaotic attractor for $F$ = 587.2 mV, $f$ = 840 Hz, and these two attractors can be viewed by altering the initial conditions (turning OFF and ON the forcing source). This interesting behavior indicates that the system has initial value dependence, and depending upon the initial conditions one can observe either chaotic or nonchaotic attractors in the ($F$-$f$)-parameter space for certain parameters.

## III. Conclusion

In this present investigation, we have described the effect of an external sinusoidal excitation on the familiar Chua's autonomous circuit. We have performed a detailed experimental investigation of the chaotic phenomena in this simple experimental system. The bifurcation diagram that classifies the attractors in the ($F$-$f$)-space indicates that the regions of chaotic behavior are interspersed with periodic regions. The Poincaré map of the attractors are observed with the aid of a simple Poincaré map circuit. Significantly, the present investigation shows that this simple driven piecewise-linear circuit is endowed with a rich variety of bifurcation sequences, including new phenomena like the equal periodic bifurcation, coexistence of multiple attractors, etc. This particular circuit alone can be effectively used to study almost all bifurcation sequences reported so far. Further experimental and numerical analysis of this circuit along with noise-induced studies may further produce some interesting results. Work along these lines is in progress.

## References


[1] P. S. Linsay, "Period-doubling and chaotic behavior in a driven anharmonic oscillator," *Phys. Rev. Lett.*, vol. 47, pp. 1349-1352, Nov. 1981.

[2] U. Partitz and W. Lauterborn, "Period-doubling cascades and devil's staircases of the driven van der Pol oscillator," *Phys. Rev. A*, vol. 36, pp. 1428-1434, Aug. 1987.

[3] T. Matsumoto, L. O. Chua, and M. Komuro, "The double scroll bifurcations," *Int. J. Circuit Theory Appl.*, vol. 14, pp. 117-146, 1986.

[4] L. O. Chua, M. Komuro, and T. Matsumoto, "The double scroll families, parts I and II," *IEEE Trans. Circuits Syst.*, vol. CAS-33, pp. 1072-1118, Nov. 1986.

[5] K. Murali and M. Lakshmanan, "Observation of many bifurcation sequences in a driven piecewise-linear circuit," *Phys. Lett. A*, vol. 151, pp. 412-419, 1990.

[6] L. O. Chua, C. A. Desoer, and E. S. Kuh, *Linear and Nonlinear Circuits.* Singapore: McGraw-Hill, 1987.

[7] L. O. Chua, Y. Yao, and Q. Yang, "Devil's staircase route to chaos in a nonlinear circuit," *Int. J. Circuit Theory Appl.*, vol. 14, pp. 315-329, 1986.

[8] M. P. Kennedy, K. R. Krieg, and L. O. Chua, "The devil's staircase: The electrical engineer's fractal," *IEEE Trans. Circuits Syst.*, vol. CAS-36, pp. 1133-1139, Aug. 1989.

[9] K. Kaneko, *Collapse of Tori and Genesis of Chaos in Dissipative Systems.* Singapore: World Scientific, 1986.

[10] Z. Su, R. W. Rollins, and E. R. Hunt, "Universal properties of the onset of chaos in diode resonator systems," *Phys. Rev. A*, vol. 40, pp. 2689-2697, 1989.

[11] J. M. T. Thompson and H. B. Stewart, *Nonlinear Dynamics and Chaos.* Chichister: Wiley, 1988.

[12] K. Fukushima and T. Yamada, "Type-III intermittency in a coupled nonlinear LCR circuit," *J. Phys. Soc. Japan*, vol. 57, pp. 4055-4062, Nov. 1988.

[13] H. G. Schuster, *Deterministic Chaos: An Introduction.* Weinheim: Physik-Verlag, 1988.

[14] G. Qin, R. Li, D. Gong, and L. Jiang, "Equal periodic bifurcation in a real dissipative system," *Phys. Lett. A*, vol. 137, pp. 255-258, May 1989.

[15] O. Maldonao, M. Markus, and B. Hess, "Coexistence of three attractors and Hysteresis jumps in a chaotic spinning top," *Phys. Lett. A*, vol. 144, pp. 153-158, Feb. 1990.

[16] S. Rajasekar and M. Lakshmanan, "Multiple attractors and their basins of attraction of a long Josephson junction oscillator," *Phys. Lett. A*, vol. 147, pp. 264-268, July 1990.


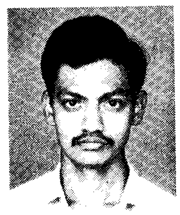

**K. Murali** received the B.Sc. degree in 1985, the M.Sc. degree in 1987, and the M.Phil degree in 1988, all in physics from Bharathidasan University, Tiruchirapalli, India.

Presently, he is working as a Dr. K. S. Krishnan Department of Atomic Energy Research Fellow towards his doctorate degree at the Centre for Nonlinear Dynamics, Department of Physics, Bharathidasan University, Tiruchirapalli, India. His main research interests are in nonlinear circuits and systems.

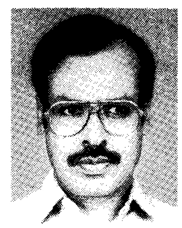

**M. Lakshmanan** received the Ph.D. degree in theoretical physics in 1974 from the University of Madras, India.

He has been associated with the Bharathidasan University, Tiruchirapalli, India since 1978, first as reader in physics (1978-84) and then as Professor of physics since 1984. His present research interests are mainly in the general area of nonlinear dynamics, particularly in the topics of solitons and chaos. He has edited/coedited the following books: *Solitons: Introduction and Applications* (Springer, 1988), *Nonlinear Evolution Equations: Integrability and Spectral Methods* (Manchester Univ. Press, 1990), and *Symmetries and Singularity Structures: Integrability and Chaos in Nonlinear Dynamical Systems* (Springer, 1991).

Dr. Lakshmanan has received several fellowships, awards and honors, including the Alexander von Humboldt Foundation Fellowship (1976), Eindhoven University of Technology Postdoctoral Fellowship (1977), Royal Society and Nuffield Foundation Bursary, U.K. (1979), Swedish Natural Science Research Council Guest Scientist Fellowship (1981), Japan Society for Promotion of Science Fellowship (1984), University Grants Commission Career Award for Young Scientists (1980), Raman Research Prize—Gold Medal, University of Madras (1980), Best University Teacher Award, Govt. of Tamilnadu (1984), and S. S. Bhatnagar prize in Physical Sciences (1989). He is a fellow of all the three Indian Academies of Sciences and a member of the National Board for Higher Mathematics, India.